Quantum tunneling of magnetization in trigonal single-molecule magnets

Junjie Liu, Enrique del Barco, and Stephen Hill

Phys. Rev. B **85**, 012406 — Published 20 January 2012

DOI: 10.1103/PhysRevB.85.012406

Quantum Tunneling of Magnetization in Trigonal Single-Molecule Magnets

Junjie Liu[1], Enrique del Barco[2] and Stephen Hill*[,3]

[1] *Department of Physics, University of Florida, Gainesville, FL 32611*
[2] *Department of Physics, University of Central Florida, Orlando, FL 32816*
[3] *Department of Physics and NHMFL, Florida State University, Tallahassee, FL 32310*

We consider quantum tunneling of magnetization (QTM) in single-molecule magnets (SMMs) possessing idealized C_3 symmetry. We do so by mapping the spectrum of a Mn_3^{III} SMM obtained via diagonalization of a multi-spin (three $s = 2$ spins) Hamiltonian onto that of a giant-spin model with spin $S = 6$. Rotation of the easy axes of the Mn^{III} atoms away from the C_3 axis leads to the emergence of the $\hat{O}_4^3$ $(\equiv \frac{1}{2}[\hat{S}_z, \hat{S}_+^3 + \hat{S}_-^3])$ operator in the giant-spin model. This unfreezes odd-k QTM resonances and generates three-fold patterns of Berry-phase interference minima in all resonances, including $k = 0$, which shifts from zero longitudinal field.

Single-molecule magnets (SMM) have attracted considerable interest during the past two decades due to landmark experiments demonstrating molecular-level magnetic bistability[1] and quantum tunneling of magnetization (QTM) at low temperatures.[2] These properties, together with the tremendous control that synthetic chemists have been able to exert over the material parameters that govern these processes, have placed SMMs as ideal platforms for understanding fundamental quantum phenomena in nanoscale magnets.[3] This letter has been motivated by recent studies of a $[NE_4]_3[Mn_3Zn_2(salox)_3O(N_3)_6Cl_2]$ SMM (hereafter Mn_3).[4-7] The molecule possesses exact C_3 point group symmetry, with a triangular core comprised of three ferromagnetically coupled Mn^{III} (s = 2) ions. The resultant spin S = 6 ground state experiences a relatively high barrier to magnetization relaxation (U_{eff} ~ 50 K). Importantly, clear evidences of quantum mechanical selection rules have been observed in QTM measurements.[6]

The Mn_3 SMM provides an ideal opportunity to explore the consequences of a trigonal spin topology in terms of the resultant QTM (for which information in the literature is scarce[8]), akin to earlier work on biaxial[9] and tetragonal systems.[10] We do so via numerical comparisons between the giant-spin approximation (GSA) and multi-spin (MS) formalism. The GSA treats the total spin S associated with the ground state of a molecule to be exact. For Mn_3, this results in $2S + 1$ (= 13) multiplet states that can be described by the following effective spin Hamiltonian:

$$\hat{H} = D\hat{S}_z^2 + B_4^0\hat{O}_4^0 + B_4^3\hat{O}_4^3 + B_6^6\hat{O}_6^6 + \mu_B \boldsymbol{B} \cdot \overleftrightarrow{g} \cdot \hat{\boldsymbol{S}} \qquad (1)$$

The first four terms characterize the so-called zero-field splitting (zfs) anisotropy. The final term represents the Zeeman interaction, with $\boldsymbol{B}$ denoting the local field and $\overleftrightarrow{g}$ the Landé g-tensor.

The $(2S + 1)$ dimension of the Hamiltonian matrix imposes a restriction on the total number of zfs operators, $\hat{O}_p^q$, where p ($\leq 2S$) is even, representing the order of the operator, and q ($\leq p$) denotes the rotational symmetry about the zero-field quantization axis (z); the B_p^q parameterize these interactions. Here, we consider only 2nd and 4th order axial (p = 2, 4; q = 0) terms, and the leading trigonal ($\hat{O}_4^3$) and hexagonal ($\hat{O}_6^6$) operators. The first term in Eq. (1) is the dominant 2nd order axial anisotropy (where $D = 3B_2^0$) that gives rise to the energy barrier between "spin up" and "spin down" states.

The advantage of the GSA lies in the fact that one need only deal with a few parameters and a small Hamiltonian matrix. However, the GSA ignores the internal degrees of freedom within the molecule, thus completely failing to capture the underlying physics in cases where the total spin can fluctuate.[7,11-14] A more physical model, which takes into account the zfs tensors of individual ions and the coupling between them, is given by the MS Hamiltonian:

$$\hat{H} = \sum_i \hat{\boldsymbol{s}}_i \cdot \overleftrightarrow{R}_i^T \cdot \overleftrightarrow{D}_i \cdot \overleftrightarrow{R}_i \cdot \hat{\boldsymbol{s}}_i + \sum_{j>i} J_{ij} \hat{\boldsymbol{s}}_i \cdot \hat{\boldsymbol{s}}_j + \sum_i \mu_B \boldsymbol{B} \cdot \overleftrightarrow{g} \cdot \hat{\boldsymbol{s}}_i \qquad (2)$$

Here, $\hat{\boldsymbol{s}}_i$ are spin operators associated with the uncoupled s = 2 Mn^{III} ions. The diagonal matrices, $\overleftrightarrow{D}_i$, parameterize the 2nd order zfs in the local coordinate frame of each Mn^{III} ion, with $D_{xx,i} = -D_{yy,i} = e_i$ and $D_{zz,i} = d_i$, where d_i $(\equiv 3B_2^0)$ and e_i $(\equiv B_2^2)$ are the respective axial and rhombic zfs parameters. The local coordinate frames are then transformed into the molecular frame by means of rotation matrices, $\overleftrightarrow{R}_i$, specified by Euler angles θ_i, φ_i and ψ_i. The second term represents the isotropic exchange between the ith and j^{th} spins, with J_{ij} parameterizing the strength of this coupling on each bond, and the final term is the Zeeman interaction.

Mn_3 is particularly attractive in the context of the present investigation. The dimension of the MS Hamiltonian matrix for three $s = 2$ spins is just $[(2s + 1)^3]^2 = 125 \times 125$. The high ($C_3$) symmetry then reduces the number of interaction parameters to just a single exchange constant, J, and identical d and e values for each ion. Two of the Euler angles are known from x-ray studies,[5] and all other important parameters have been determined from EPR and QTM measurements.[4-7] Lastly, the structure contains no solvent molecules. This is rare among SMMs[13] and removes the source of disorder.[15] Consequently, exceptional spectroscopic data (QTM and EPR) are available against which one can test theoretical models.

In this letter we focus on the transverse zfs operators in the GSA ($q > 0$), particularly $\hat{O}_4^3$, which we show to be responsible for several fascinating results. The effects of $q > 0$ zfs terms typically manifest themselves at energy scales that are orders of magnitude smaller than those of the axial ($q = 0$) terms. We thus focus on the tunneling gaps at avoided level crossings, as these are dominated by the transverse terms in Eq. (1). Due to symmetry restrictions ($q = 3n$ for C_3 symmetry, where n is an integer), non-zero tunneling gaps are limited to level crossings with $|\Delta m| = 3n$, where m is the projection of the total spin onto the C_3 (z-) axis. All such gaps, $\Delta_{mm'}$, have been labeled in Fig. 1 for QTM resonances $k \leq 3$, where k ($= m + m'$) denotes an avoided crossing between pairs of levels with spin projections m and m' (an overbar denotes negative m). Published zfs parameters were employed for simulations involving Eq. (2), i.e., d = -4.2 K and e = 0.9 K.[6] Meanwhile, the exchange constant J (= −10 K) was set to a larger absolute value to isolate the ground state from excited multiplets, thus simplifying analysis of higher-lying gaps.

The Euler angles were set to $\varphi_1 = 0$, $\varphi_2 = 120^{\circ}$ and $\varphi_3 = 240^{\circ}$ (all $\psi_i = 0$) to preserve C_3 symmetry, while θ_i (= θ) was allowed to vary in order to examine its influence on QTM selection rules.

We first consider the situation in which the Jahn-Teller (JT) axes of the three Mn^{III} ions are parallel to the C_3 axis, *i.e.*, $\theta = 0$. In the top section of Table 1, we give the magnitudes of even-n tunneling gaps involving pairs of levels with $|\Delta m_s| = 3n$, deduced via diagonalization of Eq. (2) in the absence of a transverse field, H_T ($\perp z$). The odd-n, $H_T = 0$ gaps are identically zero, as can be seen from their dependence on H_T (Fig. 1 inset): the power-law behavior indicates no contribution from zfs interactions. Consequently, one expects only even-n zfs terms of the form $B_p^{3n}\hat{O}_p^{3n}$ in the GSA: those satisfying this requirement have six-fold rotational symmetry about the C_3 axis, i.e., a higher symmetry than the real molecule (further explanation is given below).

To compare models for the $\theta = 0$ case we calculated the non-zero tunneling gaps, setting $B_4^3 = 0$, $D = -1.096$ K and $B_4^0 = -2.18\times10^{-5}$K in Eq. (1). In the absence of a transverse field, the $n = 2$ gaps $\Delta_{\bar{3}3}$ and $\Delta_{\bar{2}4}$ are proportional to B_6^6, while the $n = 4$ gap, $\Delta_{\bar{6}6}$, is proportional to $\left(B_6^6\right)^2$. This can be traced to the order of perturbation at which the gaps appear, e.g., by treating the $m_s = \pm3$ states as a two-level system, we find that $\Delta_{\bar{3}3} = B_6^6\left|\left\langle -3\left|\hat{O}_6^6\right|+3\right\rangle\right| = 60480B_6^6$ based on a first order perturbation calculation.[16] The best overall agreement between the two models is obtained by setting $B_6^6 = 4.3\times10^{-7}$K (Table 1). Small differences may be due to our neglect of higher-order six-fold terms such as $B_8^6\hat{O}_8^6$, $B_{10}^6\hat{O}_{10}^6$, *etc.*

Next we consider the situation in which the JT axes are tilted $\theta = 8.5^{\circ}$ away from the C_3 axis, as is the case for Mn_3.[5] Both even- and odd-n $H_T = 0$ tunneling gaps are generated in this

situation, i.e., odd QTM resonances become allowed. This may be understood within the framework of the GSA as being due to the emergence of zfs interactions possessing three-fold rotational symmetry about the molecular C_3 axis, i.e., $B_p^{3n}\hat{O}_p^{3n}$ with $n = 1$ and $p > 3$; the leading term is $B_4^3\hat{O}_4^3$. We begin by considering $\Delta_{\bar{1}2}$ ($k = 1$) and Δ_{03} ($k = 3$), which depend only on $B_4^3\hat{O}_4^3$ to first order. A perturbation analysis gives $\Delta_{\bar{1}2} = 132B_4^3$ and $\Delta_{03} = 368B_4^3$. By comparing with MS simulations [Eq. (2)], we obtain $B_4^3 = 4.77\times10^{-4}$ K. The remaining gaps are then evaluated via diagonalization of Eq. (1) using the optimum B_6^6 and B_4^3 parameters. Excellent agreement is once again achieved (see Table 1). Minor deviations may, in principle, be corrected by introducing higher-order transverse terms such as $B_6^3\hat{O}_6^3$.

The emergence of the $B_4^3\hat{O}_4^3$ interaction clearly signifies a lowering of the symmetry of the zfs Hamiltonian upon tilting the JT axes. To understand this one needs to consider both the symmetry of the molecule and the intrinsic symmetry of the zfs tensors of the individual ions. Considering only 2nd order zfs, the Hamiltonian of a single Mn^{III} ion possesses D_{2h} symmetry, with three mutually orthogonal C_2 axes. When the JT axes are parallel ($\theta = 0$), the local z-axis of each Mn^{III} coincides with the molecular C_3 axis. The resultant zfs Hamiltonian then possesses $C_3 \times C_2 \times C_i = C_{6h}$ symmetry (see Fig. 2a), requiring $B_4^3 = 0$; the additional C_i symmetry arises from the time-reversal invariance of Eq. (1) that guarantees an identical spectrum upon inversion of the total field (or, in the classical limit, inversion of the total spin). In contrast, when the JT axes are tilted, the C_2 and C_3 axes do not coincide. The rotational symmetry then reduces to three-fold and, hence, $B_4^3\hat{O}_4^3$ is allowed; the symmetry in this case is $C_3 \times C_i = S_6$ (see Fig. 2b).

The preceding arguments may be reinforced via group theoretic considerations without involving an exact expression of the Hamiltonian. When the external magnetic field is applied along the molecular z-axis, the C_{6h} symmetry reduces to C_6, and the 13 basis functions of the $S = 6$ Hilbert space fall into six distinct one-dimensional irreducible representations.[17] By investigating how these basis functions behave under a C_6 rotation, we can sort them as follows: $|-6\rangle, |0\rangle, |+6\rangle \in \Gamma_1$; $|-2\rangle, |+4\rangle \in \Gamma_2$; $|+2\rangle, |-4\rangle \in \Gamma_3$; $|-3\rangle, |+3\rangle \in \Gamma_4$; $|+1\rangle, |-5\rangle \in \Gamma_5$; $|-1\rangle, |+5\rangle \in \Gamma_6$; where $\Gamma_1 \ldots \Gamma_6$ are the six irreducible representations following the Bethe notation.[17] Because the Hamiltonian operator belongs to the totally symmetric representation, $\langle m|\hat{H}|m'\rangle$ is non-zero only when $|m\rangle$ and $|m'\rangle$ belong to the same representation.[18] As can be seen, such states have $|\Delta m_s| = 3n$, with n even, which is the criterion for state mixing in C_6 symmetry. When the symmetry of the zfs Hamiltonian is reduced to S_6 (C_3 upon application of $B//z$) the basis functions fall into three different irreducible representations: $|0\rangle, |\pm 3\rangle, |\pm 6\rangle \in \Gamma_1$; $|+4\rangle, |+1\rangle, |-2\rangle, |-5\rangle \in \Gamma_2$ and $|+5\rangle, |+2\rangle, |-1\rangle, |-4\rangle \in \Gamma_3$. Here, the selection rule for mixing is $|\Delta m_s| = 3n$, again in agreement with the above calculations.

An important consequence of the preceding analysis is the demonstration of the existence of odd k QTM resonances, i.e., a quite realistic parameterization of Eq. (2) generates zfs terms in the GSA containing odd powers of $\hat{S}_+$ and $\hat{S}_-$. This dispels the notion that odd QTM resonances *cannot* be generated via zfs interactions.[19] These ideas ought to apply quite generally, e.g., the disorder potential associated with the distortion of a symmetric molecule likely contains zfs terms (e.g. $\hat{O}_4^3$) that unfreeze odd QTM resonances. It remains to be seen whether this can

account for the absence of selection rules in SMMs such as Mn_{12}.[19] We note also that these arguments do not apply to zero-field ($k = 0$) QTM in half-integer spin systems, which is strictly forbidden according to Kramers' theorem.[8]

We conclude by focusing on the dependence of the tunneling gaps generated by $\hat{O}_6^6$ and $\hat{O}_4^3$ as a function of the transverse field (H_T) and its orientation within the *xy*-plane. The influence of the former is rather straightforward: the C_{6h} symmetry (see Fig. 2a) guarantees a six-fold azimuthal modulation of the tunneling gaps in all allowed resonances (not shown), regardless of whether a longitudinal field, H_L (//*z*), is present; $\hat{O}_6^6$ also generates hexagonal Berry-phase interference (BPI) patterns (due to quenching of the tunneling[6,9,10]) upon rotation of H_T within the *xy*-plane (not shown).

By contrast, the influence of $\hat{O}_4^3$ is quite fascinating. In order to simplify the discussion, Figs. 2c and 3 were generated with $B_6^6 = 0$. We first examine the dependence of $\Delta_{\bar{6}6}$ ($k = 0$) and $\Delta_{\bar{3}6}$ ($k = 3$) for a fixed value of H_T (see Fig. 2c). As anticipated, $\Delta_{\bar{3}6}$ exhibits a three-fold modulation which rotates 60° upon inversion of H_L (dashed curves), as required on the basis of the time-reversal invariance of Eq. (1), i.e., $\Delta_{\bar{3}6}$ is invariant to inversion of the total field. The figure does not convey the fact that it was also necessary to vary H_L in order to exactly locate the gap minima, i.e., H_T influences the exact H_L locations of the resonances, a behavior that is well documented for $k > 0$ resonances observed for other SMMs. The corresponding modulation of H_L also exhibits a three-fold pattern (not shown) for either polarity.

The behavior of $\Delta_{\bar{6}6}$ is yet more intriguing. One might expect a six-fold behavior given

the requirement that the spectrum be invariant under inversion of H_T. However, this assumes that $H_L = 0$. In fact, application of a transverse field causes a shift of the $k = 0$ resonance away from $H_L = 0$, as illustrated in Fig. 2d. Only a very weak modulation of $\Delta_{\bar{6}6}$ is observed upon rotation of a 0.2 T transverse field; the modulation pattern is indeed six-fold (solid curve in Fig. 2c). However, the corresponding modulation of H_L exhibits a three-fold pattern (dotted and dash-dotted curves in Fig. 2c). One way to interpret this result is to view the $\hat{O}_4^3$ operator as generating an effective internal longitudinal field, H_L^*, under the action of an applied transverse field; H_L^* is then responsible for the shift of the $k = 0$ resonance from $H_L = 0$. Indeed, one can see this from inspection of the form of the $\hat{O}_4^3$ $\left(= \frac{1}{2}\left[\hat{S}_z, \hat{S}_+^3 + \hat{S}_-^3\right]\right)$ operator, which, unlike even-q interactions, contains an odd power of $\hat{S}_z$, akin to the Zeeman interaction with $H//z$. An alternative view may be derived from the S_6 surface depicted in Fig. 2b, where one sees that the hard/medium directions do not lie within the xy-plane, contrary to the case for the C_{6h} surface in Fig. 2a (or quite generally for any even-q operator[20]). In other words, the classical hard plane is not flat, but corrugated with a 120° periodicity. Consequently, application of a longitudinal field is required in order to insure that the total field is within the hard plane when rotating H_T.

Finally, Fig. 3 shows the patterns of BPI minima for $k = 0$ (a) and $k = 3$ (b), generated purely from the $B_4^3\hat{O}_4^3$ interaction. The $k = 0$ pattern in (a) is hexagonal. However, the polarity of the compensating longitudinal field, H_L (represented by color and +/- symbols), alternates between successive minima. Therefore, on this basis, one concludes that the BPI minima exhibit a three-fold rotational symmetry. In contrast, the $k = 3$ BPI minima exhibit obvious trigonal

patterns, regardless of the behavior of the compensating H_L field. Observation of these BPI patterns in Mn_3 is complicated by several factors, including strong avalanches[6] and the existence of two molecular orientations (with parallel C_3 axes);[4,5] we note that it may be possible to select and study one species via hole-burning.[21] The primary motivation for the present theoretical study is to stimulate future measurements on Mn_3 or one of several other SMMs known to possess C_3 symmetry.[8]

Acknowledgements:

This work was supported by the NSF, grant nos DMR-0747587 (EdB) and 0804408 (SH). The NHMFL is supported by the NSF (DMR-0654118) and the State of Florida.

References:

* Email: shill@magnet.fsu.edu

[1] A. D. Caneschi et al., J. Am. Chem. Soc. **113**, 5873 (1991).

[2] J. R. Friedman, M. P. Sarachik, J. Tejada, R. Ziolo, Phys. Rev. Lett. **76**, 3830 (1996).

[3] D. Gatteschi, R. Sessoli, and J. Villain, *Molecular Nanomagnets* (Oxford University Press, Oxford, 2006).

[4] P. L. Feng et al., Inorg. Chem. **47**, 8610 (2008).

[5] P. L. Feng et al., Inorg. Chem. **48**, 3480 (2009).

[6] J. J. Henderson et al., Phys. Rev. Lett. **103**, 017202 (2009).

[7] S. Hill et al., Dalton Trans. **39**, 4693 (2010).

[8] W. Wernsdorfer et al., Phys. Rev. B **65**, 180403 (2002).

[9] W. Wernsdorfer, R. Sessoli, Science **284**, 133 (1999).

[10] C.-S. Park, A. Garg, Phys. Rev. B **65**, 064411 (2002).

[11] W. Wernsdorfer et al., Nature **416**, 406 (2002).

[12] S. Carretta et al., Phys. Rev. Lett. **92**, 207205 (2004).

[13] A. Wilson et al., Phys. Rev. B **74**, 140403 (2006).

[14] C. M. Ramsey et al., Nat. Phys. **4**, 277 (2008).

[15] G. Redler et al., Phys. Rev. B **80**, 094408 (2009).

[16] We note that the tunneling gaps are related to J (see [7]), e.g., $B_4^3 \propto |J|^{-1}$ & $B_6^6 \propto |J|^{-2}$, implying a complete suppression of QTM in the strong coupling limit ($|J| \gg |d|$).

[17] J. O. D. George F. Koster, Pobert G. Wheeler and Hermann Statz, *Properties of the Thirty-Two Point Groups* (M.I.T. Press, Cambridge, MA, 1963).

[18] F. A. Cotton, *Chemical Applications of Group Theory* (A Wiley-Interscience Publication,

1990).

[19] J. van Slageren et al., Phys. Rev. B **79**, 224406 (2009).

[20] F. Li, A. Garg, Phys. Rev. B **83**, 132401 (2011).

[21] E. del Barco et al., J. Low. Temp. Phys. **140**, 119 (2005).

k	n	Δ	GSA gap – Eq. (1) (K)	MS gap – Eq. (2) (K)	Ratio (GS/MS)
Jahn-Teller axes parallel to the molecular z-axis					
0	2	$\Delta_{\bar{3}3}$	2.60×10^{-2}	2.66×10^{-2}	0.98
0	4	$\Delta_{\bar{6}6}$	1.10×10^{-6}	1.05×10^{-6}	1.05
2	2	$\Delta_{\bar{2}4}$	2.37×10^{-2}	2.35×10^{-2}	1.01
Jahn-Teller axes tilted $\theta = 8.5^o$ away from the molecular z-axis					
0	2	$\Delta_{\bar{3}3}$	2.76×10^{-2}	2.91×10^{-2}	0.95
0	4	$\Delta_{\bar{6}6}$	1.26×10^{-6}	1.25×10^{-6}	1.01
1	3	$\Delta_{\bar{4}5}$	4.68×10^{-5}	4.19×10^{-5}	1.12
1	1	$\Delta_{\bar{1}2}$	6.33×10^{-2}	6.31×10^{-2}	1.00
2	2	$\Delta_{\bar{2}4}$	2.45×10^{-2}	2.61×10^{-2}	0.94
3	3	$\Delta_{\bar{3}6}$	8.66×10^{-5}	7.53×10^{-5}	1.15
3	1	Δ_{03}	1.76×10^{-1}	1.76×10^{-1}	1.00

Table 1: Comparison of tunneling gaps obtained from the MS and GSA models for resonances k = 0, 1, 2 and 3, for the two cases $\theta = 0$ (top) and $\theta = 8.5^{\circ}$ (bottom).

Figure captions

Fig. 1. (color online) Zeeman diagram for a spin $S = 6$ multiplet with easy-axis anisotropy [$D < 0$ in Eqn. (1)] and $H//z$. All possible non-zero tunneling gaps for C_3 symmetry are labeled according to the scheme discussed in the main text. The inset shows the H_T dependence of the odd-n tunneling gaps.

Fig. 2. (color online) Potential energy surfaces corresponding to the $\hat{O}_6^6$ (a) and $\hat{O}_4^3$ (b) GSA operator equivalents. (c) $k = 0$ (solid curve) and $k = 3$ (dashed curves) ground state tunneling gaps as a function of the orientation of H_T (= 0.2 T) within the xy-plane, calculated using Eqn. (1) with $B_6^6 = 0$. The data have been normalized and offset to aid viewing: $\Delta_{\bar{3}6}$ oscillates from 3.65 to 3.90×10^{-6} K (~6%) and $\Delta_{\bar{6}6}$ from 4.065 to 4.074×10^{-9} K (~0.2%). The inner curves correspond to the H_L field (dotted $\Rightarrow H_L > 0$, dash-dotted $\Rightarrow H_L < 0$) needed to compensate for the shift of the $k = 0$ resonance upon application of H_T as illustrated in (d): for $H_T = 0.2$ T, H_L oscillates about zero with an amplitude of 6.3×10^{-7} T and a three-fold (S_6) periodicity.

Fig. 3. (color online) Contour plots of $\Delta_{\bar{6}6}$ (a) and $\Delta_{\bar{3}6}$ (b) as a function of H_T, calculated using Eqn. (1) with $B_6^6 = 0$. A compensating H_L field was required in (a) that alternates between positive (+) and negative (-) values. Both figures display BPI minima (dark spots) that exhibit three-fold symmetry when the variation of H_L is also taken into account.

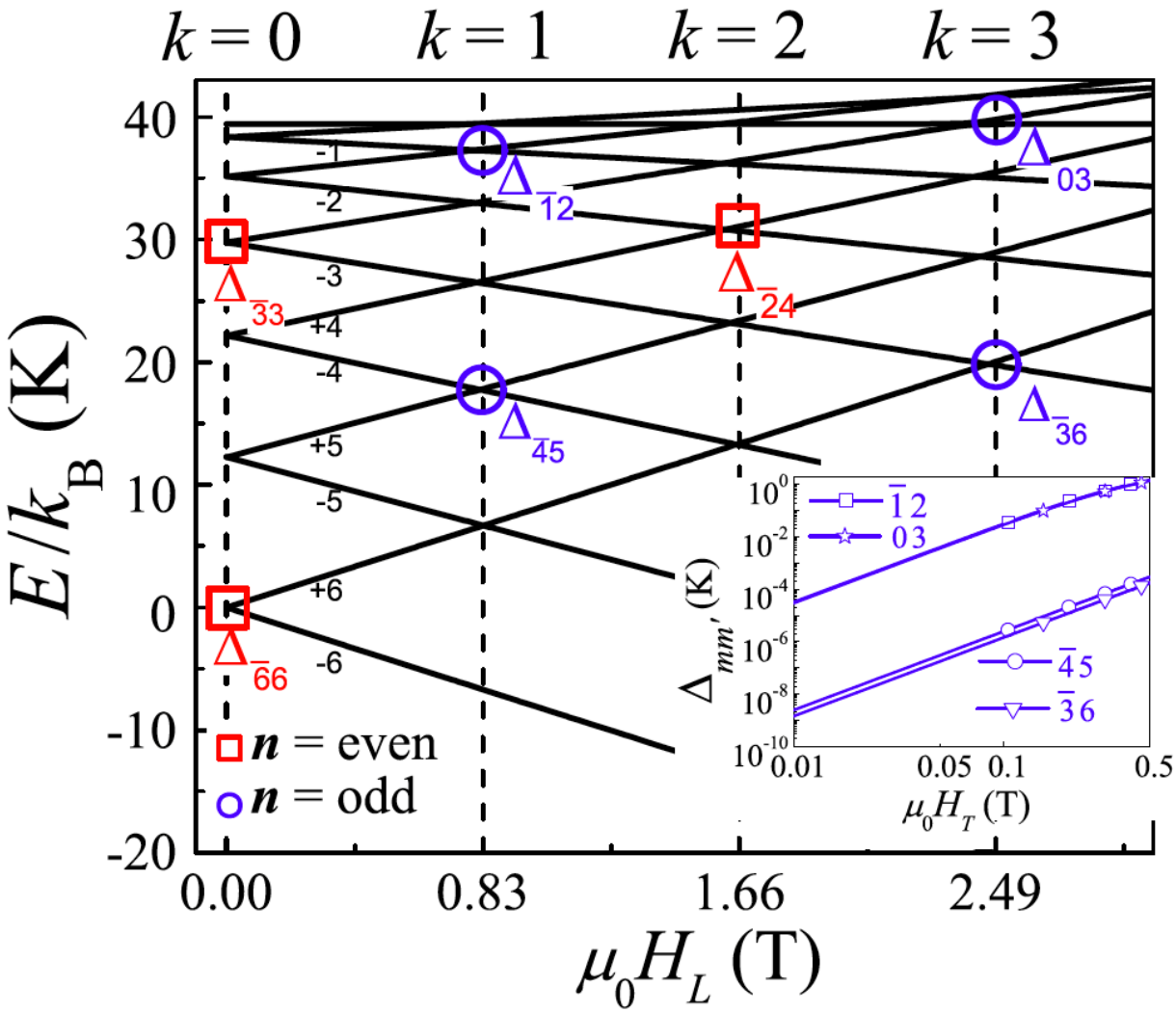

Liu et al., Figure 1

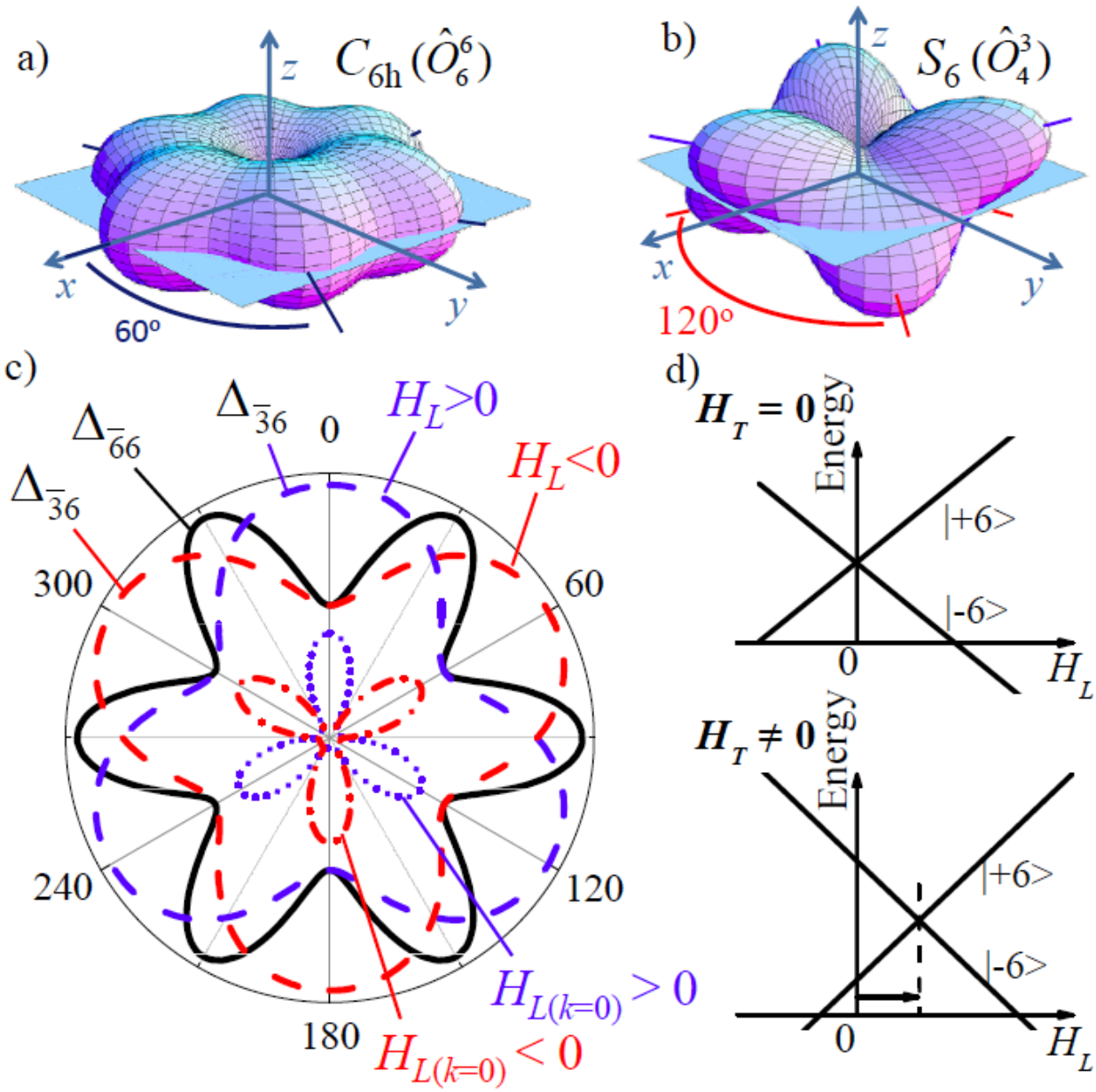

Liu et al., Figure 2

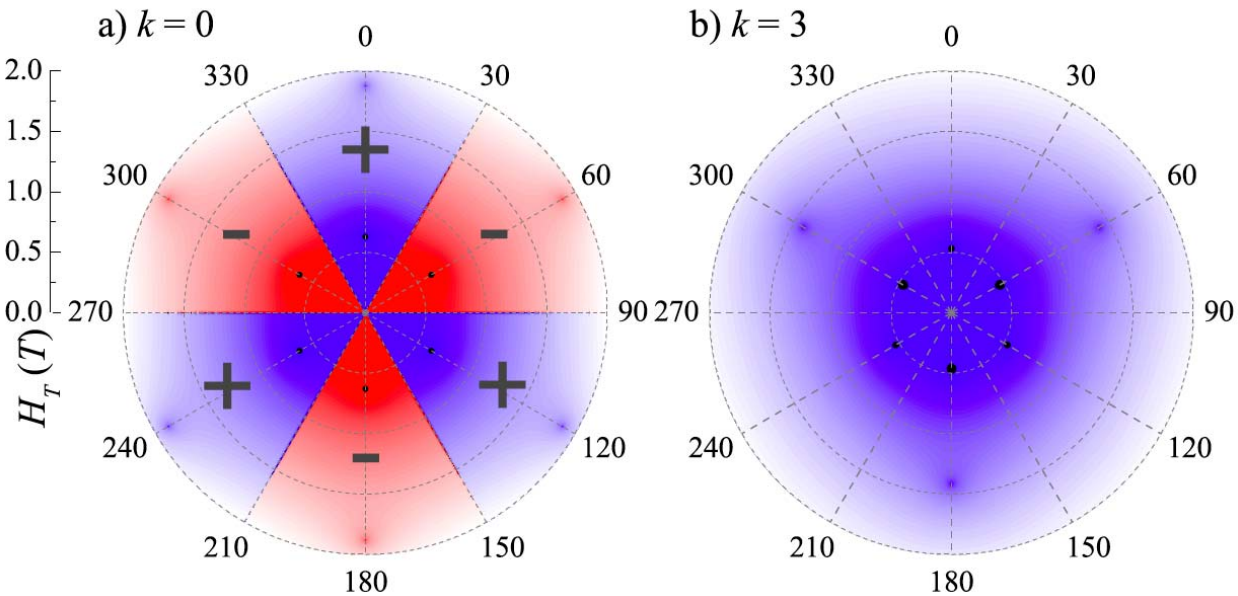

Liu et al., Figure 3